Available online at www.sciencedirect.com
SCIENCE DIRECT®
Journal of Sound and Vibration 288 (2005) 463–486
JOURNAL OF SOUND AND VIBRATION
www.elsevier.com/locate/jsvi

A fuzzy finite element procedure for the calculation of uncertain frequency response functions of damped structures: Part 2—Numerical case studies

Hilde De Gersem*, David Moens, Wim Desmet, Dirk Vandepitte

K.U. Leuven, Department of Mechanical Engineering, PMA, Celestijnenlaan 300B, B-3001 Heverlee, Belgium

Accepted 5 July 2005
Available online 2 September 2005

Abstract

This work introduces a numerical algorithm to calculate frequency response functions of damped finite element models with fuzzy uncertain parameters. Part 1 of this paper focusses on the numerical procedure for the solution of the underlying interval finite element problem, based on the undamped procedure and the principle of Rayleigh damping. Part 2 of this paper illustrates the applicability of the methodology through four case studies. The concepts of the interval and the fuzzy finite element frequency response function analysis are illustrated for different types of uncertainties. The obtained results are compared with the results of Monte Carlo simulations.

1. Introduction

1.1. The fuzzy finite element method

In this paper a non-probabilistic, fuzzy finite element (FFE) method is presented for the calculation of frequency response functions (FRFs) of mechanical structures with uncertain parameters. The concept of fuzzy numbers and membership functions is used to describe subjective and incomplete uncertainty data. Based on this concept and the principle of

*Corresponding author. Tel.: +32 16 32 86 06; fax: +32 16 321 985.
E-mail address: hilde.degersem@mech.kuleuven.ac.be (H. De Gersem).

0022-460X/$ - see front matter © 2005 Elsevier Ltd. All rights reserved.
doi:10.1016/j.jsv.2005.07.002

modal superposition, a numerical procedure for the calculation of interval and fuzzy FRFs is developed [1,2].

The description of an uncertain parameter using a membership function can practically be implemented using the *α-level strategy*. This approach subdivides the membership function range into a number of α-levels. The intersection with the membership function of the input uncertainties at each α-level results in an interval $x_{i,\alpha}^{I} = [\underline{x}_i, \overline{x}_i]_\alpha$. With these input intervals of the α-sublevel, an interval finite element (IFE) analysis is performed, resulting in an interval for the analysis result at the considered α-level. Finally, the fuzzy solution is assembled from the resulting intervals at each sublevel.

Part 1 of this paper concentrates on the numerical algorithm developed to solve the underlying IFE problem. The basic method, named the *Modal Rectangle* (MR) method, is an interval translation of the deterministic modal superposition principle and consists of three successive steps. First the correct intervals on the modal mass and stiffness parameters of all considered modes are calculated using a global optimisation procedure. Subsequently the interval modal contributions of each individual mode to the total response function are determined. Finally, the summation of all individual contributions results in the total interval FRF. An enhancement of this method is obtained by taking the correct eigenvalue intervals into account during the calculation of the individual modal FRF contributions, resulting in the *Modal Rectangle method with Eigenvalue interval correction* (MRE). These concepts and methods are extensively described in part 1 of this paper.

This part illustrates the applicability of the interval and the FFE method through four case studies. First the influence of uncertain, non-ideal boundary conditions on the dynamic behaviour of a simple rectangular plate is investigated. Next, interval and fuzzy FRF results for the Garteur benchmark aircraft model with three different types of uncertainties are presented. The third case study consists of a solar panel for which the influence of geometric uncertainties on the dynamic displacements of the panel tips is investigated. Finally, the influence of uncertainties on the eigenfrequencies and a direct FRF of the COROT telescope baffle cover is determined.

1.2. Definitions of variability and uncertainty

In literature, the use of the terminology *uncertainty* and *variability* is not unambiguous. Different researchers apply the same terminology but the meaning attached to these is rather inconsistent. This necessitates a profound clarification of the terminology for each publication which treats uncertainties. This paper does not propose a new terminology, but applies the terminology proposed by Oberkampf [3], who describes the total uncertainty in computational simulations that deal with the numerical solution of a system of partial differential equations. Some additional nuances are, however, necessary in order to enable clear distinction between probabilistic and non-probabilistic quantities in this paper. See Ref. [4] for a survey of sources of variability and uncertainty in general FE analysis.

The term *variability* covers *the variation which is inherent to the modelled physical system or the environment under consideration*. Generally, this is described by a distributed quantity defined over a range of possible values. The exact value is known to be within this range, but it will vary from unit to unit or from time to time. Ideally, objective information on both the range and the likelihood of the quantity within this range is available. Some literature refers to this variability as

aleatory uncertainty or *irreducible uncertainty*, referring to the fact that even when all information on the particular property is available, the quantity cannot be deterministically determined. Typical examples of variability are:

- a property of a design which is subject to manufacturing tolerances;
- environmental effects on a model (temperature, humidity, ...);
- properties of non-uniform materials;
- identifiable disturbances in operating conditions.

An *uncertainty* is *a potential deficiency in any phase or activity of the modelling process that is due to lack of knowledge*. The word *potential* stresses that the deficiency may or may not occur. This means that there may be no deficiency even though there is some lack of knowledge, i.e. when the numerical model of the phenomenon happens to be correct rather by chance than due to exact knowledge. Possibly, limited objective information is available, for instance when a range of possible values is known. In most cases, however, information on uncertainties is subjective and based on some expert opinion. Other sources in literature refer to this uncertainty as *reducible*, *epistemic* or *subjective uncertainty*. Typical examples of uncertainties are:

- non-rigid models for boundary conditions;
- simplified models for joints;
- models for material damping;
- unpredictable model changes due to ageing, loading, ...

Table 1 summarises the definitions in this section with their main characteristics in the context of the FE methodology.

The definitions of uncertainty and variability according to Oberkampf are rather straightforward and comprehensible, but they are not mutually exclusive. A variability could be subject to lack of knowledge, as information on its range or likelihood within the range could be missing. This is for instance the case for every design dimension subject to tolerances, but without further specification of manufacturing process. The tolerances represent the bounds on the feasible domain, but give no information on likelihood within these bounds. In this case, the information is insufficient to exactly describe the variability, in other words, there is a lack of knowledge. Consequently, such a variability is also an uncertainty. It is referred to here as an *uncertain*

Table 1
Overview of the main characteristics of the definitions of variability and uncertainty

Variability	• Corresponds to a variation in a model property which actually occurs in the physical design • Irreducible • Ranges over time or from unit to unit
Uncertainty	• Corresponds to any model property that cannot be quantified exactly • Reducible through increasing knowledge • Represents a lack of knowledge

variability. Opposed to the uncertain variability, a *certain variability* refers to a variability the range and likelihood of which are exactly known.

In numerical modelling practice, the majority of model properties are implemented as constant deterministic values. Though most of them are subject to variation, the influence of their variability on the analysis result is considered to be negligible. Often, uncertainties refer to a possible lack of knowledge in these deterministic properties rather than a variability from unit to unit or in time in the final product. This type of uncertainty is referred to as *invariable uncertainty*. The invariable uncertainties typically occur in model properties for model parts or external influences on the model which are difficult to describe numerically, but considered constant in the final physical product (connections, damping, ...). Other examples are design properties which have negligible variability but which are not defined exactly in an early design stage.

1.3. Probabilistic versus possibilistic uncertainty assessment

The case studies that are considered in this paper are selected to illustrate different types of uncertainty on finite element (FE) model parameters. The probabilistic Monte Carlo simulation (MCS) method is the best known procedure to investigate the influence of variabilities on the static and dynamic behaviour of structures. This method is particularly suitable for FE models with certain variabilities, which occur typically in advanced stages of the design process. However, the use of the MCS method can lead to subjective results when not all statistical data are available and assumptions on the probability density functions of the uncertain parameters have to be made. The case studies presented in this paper show that possibilistic approaches are complementary to probabilistic approaches. Although possibilistic approaches are able to describe problems of certain variability to a certain extent, yet without statistical interpretation, the added value of possibilistic approaches is mainly in problems where incomplete information is available, i.e. in the case of invariable uncertainties and uncertain variabilities. This situation occurs typically in the early stage of product design procedures when some design parameters are not yet fixed. Other conditions that can be handled with a possibilistic approach occur when model parameters simply cannot be determined because insufficient information can be gathered.

Although probabilistic analysis is not really feasible for the cases that are discussed below as no information on the likelihood within the interval bounds is available, Monte Carlo analyses have been performed simply for the sake of comparison of results. Uniform distributions are assumed for parameters that are known only by their lower and upper bounds. The number of Monte Carlo samples used in this paper is rather small because of the limited size of the models and the limited number of uncertain parameters. The number of runs required to obtain reliable results increases exponentially with the number of uncertain parameters and the model size. Consequently, the MCS method becomes very time consuming for industrially sized models. Furthermore, the number of samples needed is hard to predict as the relation between the uncertain parameters and the responses can be highly nonlinear. It should also be emphasised that the MCS method, as opposed to the anti-optimisation strategy, does not explicitly search for the worst-case scenario, i.e. the situation for which the response of the structure reaches its maximum or minimum. It is unlikely that the Monte Carlo analysis results include the samples which yield the exact bounds on the analysis result. Therefore, the comparison of interval FE results with the results of a MCS gives only a qualitative indication of the bounds obtained by the IFE procedure.

1.4. Vertex analysis

It can be shown easily that vertex analysis correctly predicts the intervals of output quantities if the problem is monotonic. This condition is met when the relation between all uncertain input parameters and the output quantity is monotonic. The minimum and maximum value of the output quantity are found with a combination of minimum and maximum values on each individual input parameter. In these conditions, it is sufficient to take all (2^n) possible combinations of n uncertain input parameters to calculate the extreme value of the output quantity. This concept is developed in the basic version of the transformation method [5,6]. In another terminology, it is the full factorial analysis from the design of experiments methodology. In the application of structural dynamics, it is however impossible to prove the property of monotonicity in a general way. Experience shows that many problems do exhibit indeed a monotonic behaviour, especially when global model parameters are uncertain. It is intuitively clear that an increase of the Young's modulus that is constant throughout the structure stiffens the structure, with an increase of resonance frequencies by a factor equal to the square root of the multiplication factor on the modulus. For other model parameters, especially if they affect only part of the structure, it is much harder to predict the effect of a parameter change. It is therefore necessary to apply a global optimisation procedure in search of maximum response values. The second case study is specifically selected to show that parameter dependency may be non-monotonic.

2. Case study I: plate with uncertain boundary conditions

2.1. Model description

In a first case study, special attention is paid to the analysis of a structure with uncertain boundary conditions. Three types of conditions are commonly applied: free, pinned (prescribed displacements) or fixed (prescribed displacements and rotations). Whereas free boundary conditions are usually correctly represented, both other conditions are only approximations of physical reality. A prescribed value of displacement and/or rotation corresponds to an infinite stiffness of the relevant degree of freedom (dofs). In reality, the boundary stiffness is always finite, yet with an unknown or uncontrollable value.

This case study shows that the concepts of the IFE method and the FFE method can be applied in a dynamic analysis taking uncertain boundary conditions into account. The studied model is a rectangular plate which is clamped at one edge as illustrated in Fig. 1 [2]. A damped interval and fuzzy FRF analysis is performed between the translational dofs of the free corner nodes of the plate, as indicated in the figure. The reference FE model consists of 100 pure bending plate elements, implemented using the thin plate model according to the KIRCHHOFF plate theory. The properties of the deterministic FE model are listed in Table 2.

Whereas in FE models a clamping is usually modelled with an infinite clamping stiffness and zero displacements, this does not correspond to reality in which an ideal clamping stiffness does not exist. In this case study, finite stiffness clamping boundary conditions are modelled using linear springs between the boundary nodes of the plate and the environment at the clamped edge.

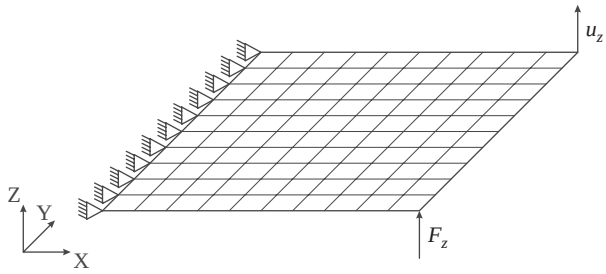

Fig. 1. Finite element model of the clamped plate.

Table 2
Properties of the deterministic FE model of the rectangular plate

Young's modulus	210 GPa
Poisson constant	0.3
Mass density	7800 kg/m^3
Dimension	1 m × 1 m
Thickness	0.005 m

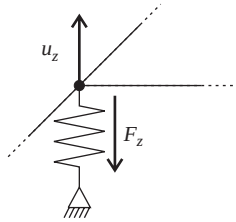

Fig. 2. Finite stiffness spring for a translational dofs at the clamped edge.

This is illustrated for a translational dofs in Fig. 2. The introduction of these springs allows a non-zero translation at the clamped edge. As indicated in Fig. 2, a spring introduces an external load on a node equal to $F_z = -k_z u_z$, with k_z the stiffness coefficient of the linear spring. A similar procedure can be applied to introduce a finite stiffness on the clamping of the rotational dofs.

2.2. Damped interval and fuzzy FRF analysis

The precise value of the boundary stiffness is unknown. It would even be hardly feasible to measure it. Depending on the type of clamping device, it may even be variable over the length of the edge. A typical characteristic of possibilistic analysis is that knowledge of upper and lower bounds are sufficient to predict the bounds on dynamic response. The actual bounds on the input parameters have to be determined from engineering judgement.

A damped interval FRF analysis is performed on the plate with uncertain translational spring stiffnesses k_z ranging between 0.4 and 40 MN/m, while the rotational clamping stiffness remains

infinite. In this model one translational spring is applied with a constant imprecise value at each of the 11 boundary nodes. The spring stiffness values are selected to actually affect the dynamic behaviour of the clamped plate. For modes 1–6, eigenvalue sensitivity to spring stiffness is small, and the mode shapes are very similar with any spring stiffness within the specified range. For modes 7 and beyond, not only the resonance frequencies but also the mode shapes change with changing spring stiffness. With the upper bound of k_z, the supported edge does not displace in mode 7. With k_z values lower than 40 MN/m, edge displacements do occur for modes 7 and beyond. Resonance frequencies and mode shapes are most sensitive to the translational spring stiffness for modes 7 and 9.

During the FRF analysis nine eigenmodes are taken into account, covering a frequency range up to 100 Hz. The damping ratios of all considered modes are taken to be between 0.7% and 1.9%. Three different analysis runs have been performed:

1. an interval analysis using the MRE method;
2. a MCS with 100 samples generated from a uniform distribution on the (linear) interval $k_z = [0.4; 40]\,\mathrm{MN/m}$;
3. a MCS with 100 samples generated from a uniform distribution on the interval of $\log k_z = [5.6; 7.6]\,\mathrm{N/m}$.

Fig. 3(a) illustrates the envelope FRF resulting from an interval analysis using the MRE strategy (run 1), compared to the results of run 2. This figure shows some regions where the envelope FRF does not give a narrow circumscription of the Monte Carlo samples. For instance, between 70 and 73 Hz, the correspondence between the upper bound from the interval FRF analysis and the MC samples is bad. At this point, it is impossible to say whether this is due to either conservatism of the MRE method or inadequate sampling in the MCS. The other MCS (run 3) results in a much

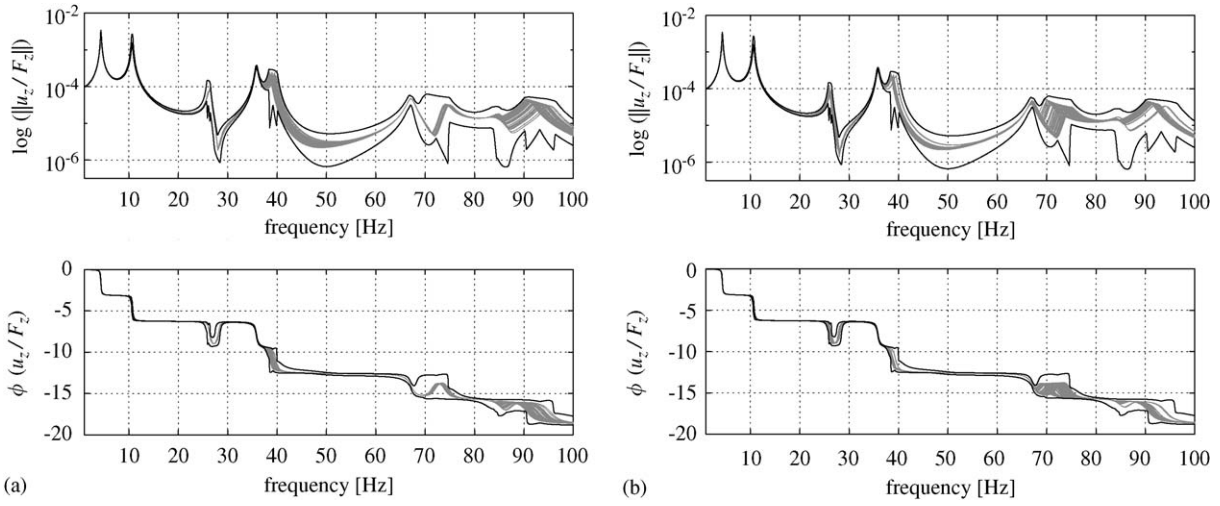

Fig. 3. Amplitude and phase envelopes of a damped interval FRF (MRE method, black lines), compared with the results of a MCS with 100 samples (grey lines): (a) uniform Monte Carlo sampling; (b) uniform logarithmic Monte Carlo sampling.

better correspondence in this specific frequency region as illustrated in Fig. 3(b). However, the correspondence is now worse in the frequency region between 95 and 97 Hz. This shows that the response range covered with the MCS is strongly affected by the choice of the probability density function (PDF) on the considered interval.

A MCS with uniform distribution on the logarithm of the input uncertainty interval results in more samples close to the lower bound of the interval. Consequently, the MCS gives a better approximation of the response range in frequency regions where the FRF is mainly determined by a mode that is to a large extent affected by the lower bound of the input uncertainty interval. This phenomenon occurs in the frequency range between 70 and 73 Hz (mode 7). The opposite phenomenon is detected in the frequency range between 95 and 97 Hz, where the FRF range is determined by mode 9, which is mainly affected by the higher values of the spring stiffness. Therefore, the MCS with uniform distribution gives a better approximation of the correct response range in this frequency region.

We can conclude that the IFE envelope FRF returns a solution guaranteed to contain the true response range after a single run. In this case study the MCS requires several sampling strategies in order to cover adequately the response range in the total frequency domain. Unless a priori knowledge is available, the interpretation of probabilistic FRF results would be misleading if only one of the two Monte Carlo sampling strategies were considered.

Fig. 3 also shows that in the frequency ranges around 50 Hz and around 80 Hz the amplitude of the FRF bounds calculated with the MRE method are significantly more conservative with respect to the MCS results. In general there are three sources of conservatism in the MRE method (cf. Part 1). First, conservatism in the modal real and imaginary envelope FRF is introduced by the conservatism in the $\langle \hat{k}_i, \hat{m}_i \rangle$-domain approximation. A second source of conservatism arises from the independent summation of the modal real and imaginary parts, which neglects the correlation between the contributions of different modes. Finally, the amplitude and phase envelope FRF calculation considers the ranges on the real and imaginary part of the total response independently, while they are actually coupled through the global system. Typically, these phenomena mainly affect the FRF bounds in the frequency regions between the eigenfrequency ranges. Future research is planned to further reduce the amount of conservatism in these frequency regions.

Fig. 4 illustrates the results of a fuzzy FRF analysis using uncertain properties for the connection stiffness of the rotation clamping dofs, while the translational clamping stiffness

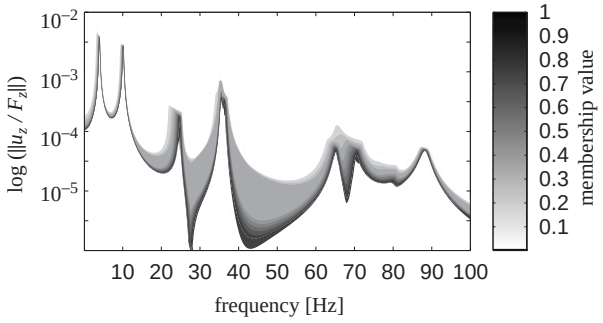

Fig. 4. Fuzzy FRF combining the IFE upper bound FRFs at 11 α-levels.

remains infinite. The fuzzy FRF is the result of the combination of the upper bounds of an IFE analysis on 11 α-levels. The fuzzy membership function of the stiffness has a symmetrical triangular shape with a linear stiffness interval between 0.1 and 10 kNm/rad at the α-level equal to zero. This figure reveals an artificial nonlinear sensitivity of the response upper bound to the stiffness interval applied on the clamped edge. This phenomenon is caused by the fact that for membership level values smaller than 0.6, two modes near 35 Hz become switch modes, for which the modal domain approximations are more conservative. This causes the interval FRF at these membership levels to be more conservative. It should however be stressed that this phenomenon only occurs in frequency regions between the resonance peaks. The interval FRF at the resonance peaks remains narrowly predicted, even when switch modes occur in the analysis.

3. Case study II: the Garteur benchmark problem

3.1. Model description

The simplified aircraft model of the Garteur benchmark problem is a common testbed designed and manufactured by the Garteur Action Group to evaluate the efficiency and reliability of different ground vibration test techniques [7,8]. It has also been used extensively for testing model updating methods and model error localisation procedures.

The structure consists of a small-scale aluminium aircraft model with a length of 1.5 m, a wing span of 2 m and a mass of 44 kg. The fuselage of the aircraft consists of a rectangular plate with a thickness of 50 mm. The aluminium tail with a thickness of 10 mm is connected rigidly to the fuselage. The wings are connected to the fuselage through an intermediate steel plate. Wingtips are rigidly connected at both ends of the wings. Both the wings and wingtips are rectangular aluminium plates with a thickness of 10 mm. A visco-elastic layer is glued onto a part of the wings. Three concentrated masses are present: one on each wingtip and one on the fuselage.

A FE model has been created based on the description of the physical model, data of the FE model made by the Garteur Action Group and test data. The model, as illustrated in Fig. 5(a), is built with 1014 CQUAD8 elements, and it contains almost 20,000 dofs [9].

The Garteur aircraft model contains some inherent uncertainties, due to a lack of knowledge on the physical model as well as due to uncertainty on the modelling level. Three uncertainties are considered during the dynamic analysis of the structure.

1. A first source of uncertainty is the visco-elastic layer, glued onto a part of the wings. The damping characteristics of this visco-elastic layer, as well as the quality of the glue connection are not exactly known. The combined structure of wing and visco-elastic layer connected by glue, is modelled using a layered material. In the performed analyses, the uncertainty on the quality of the glue connection is represented by an uncertain thickness of the visco-elastic layer between 0.1 and 1.6 mm, with a nominal value of 1.1 mm.
2. A second source of uncertainty is the stiffness of a part of the connection between the wings and the fuselage, an inherent modelling uncertainty. In the assembled model, this connection is modelled with an interconnecting plate parallel to the wings, as shown in Fig. 5(b). The fuselage is rigidly connected to this plate. The dofs of the interconnecting plate are rigidly connected to

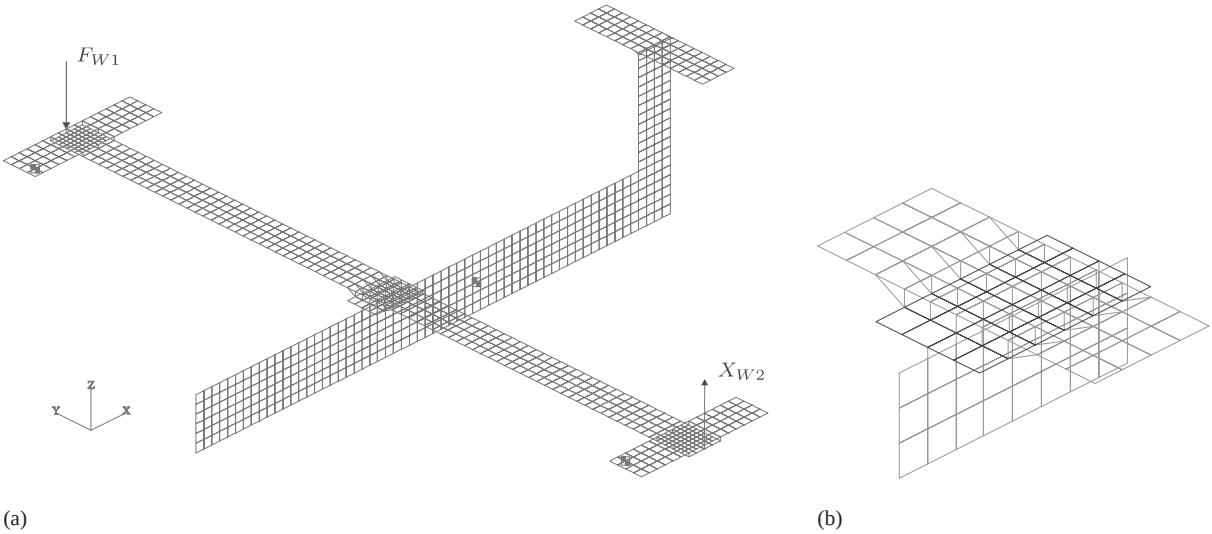

Fig. 5. Finite element model of the Garteur benchmark aircraft: (a) global FE model; (b) detail of the connection between fuselage and wings.

the wings, except for the dofs on the edge of the plate. These dofs are connected to the corresponding dofs on the wings using linear springs [9]. The dimension and the stiffness of the connection between the wings and the fuselage can then be varied in a continuous way by changing the stiffness of these springs. In the performed analyses this stiffness ranges between 10 and 10^{15} N/m with a nominal value of 10^{8} N/m. The lower bound of this uncertainty interval simulates the situation in which the edge of the connection plate does not contribute to the connection between wings and fuselage. The upper bound simulates the situation in which the corresponding dofs of the edge of the interconnecting plate and the wings are rigidly connected. An experienced engineer usually has sufficient knowledge to specify a more narrow interval. The interval $[10; 10^{15}]$ N/m is taken artificially wide here, to demonstrate the capability of the developed methods to deal with highly uncertain parameters. Of course, care should be taken not to create near-singularities in the FE model.

3. A third uncertainty is introduced on the Young's modulus of the wing material, with a range of 67.5 GPa up to 68.5 GPa, with nominal value 68.0 GPa.

These uncertainties represent three different types of uncertainty: an early design uncertainty (thickness of the visco-elastic layer), a modelling uncertainty (the connection between wings and fuselage) and a global physical uncertain variability (Young's modulus).

The influence of the uncertain parameters on the FRF between the wingtips of the aircraft model is investigated. The input and output dofs W1 and W2 are indicated in Fig. 5(a). For the calculation of the interval FRF, 14 modes are taken into account, covering a frequency range up to 160 Hz.

In Section 3.2 the influence of the thickness of the visco-elastic layer on the dynamic behaviour of the aircraft is investigated. The results for both the MR and the MRE method are presented. Section 3.3 studies the combined effect of the three considered uncertainties. The last section

presents the results of a fuzzy FRF analysis of the damped aircraft model including all three uncertain parameters.

3.2. Influence of the thickness of the visco-elastic layer

Fig. 6 presents the results of the damped interval FRF analysis calculated with the MR and the MRE methods, compared with the results of a MCS with 100 uniformly distributed samples (gray curves). The dashed black lines represent the envelope FRF calculated with the MR method, whereas the solid black lines represent the envelope FRF calculated with the MRE method. The values of the proportional damping coefficients α_K and α_M are 5×10^{-5} and 2, respectively, resulting in damping ratios between 1.0% and 2.8% for all 14 considered modes. The figure clearly shows the improvement of the envelope FRFs achieved by the MRE method. This improvement is obtained by using the correct eigenfrequency intervals for the approximation of the modal domain (cf. Fig. 7). The upper and lower bounds on the FRF, calculated with the MRE method, give a narrow circumscription of the MCS results for the entire frequency range.

Table 3 lists the corresponding eigenfrequency intervals used in the MRE method. For several modes the eigenfrequency and the modal mass and stiffness parameters behave in a non-monotonic way with respect to the thickness of the visco-elastic layer, as illustrated in Fig. 8 for mode 2. The vertex method, which only considers the boundary values of the uncertainty intervals to calculate the boundary values of the modal parameters, does not correctly predict actual boundaries on the modal parameters $\langle \hat{k}_i \rangle$, $\langle \hat{m}_i \rangle$ and $\langle f_i \rangle$. Therefore, a global optimisation procedure for the calculation of the modal parameter intervals is required.

3.3. Interval FRF analysis with three uncertain parameters

A damped IFE FRF analysis is performed, taking into account all three uncertain parameters: the thickness of the visco-elastic layer, the stiffness of the connection springs between the wings

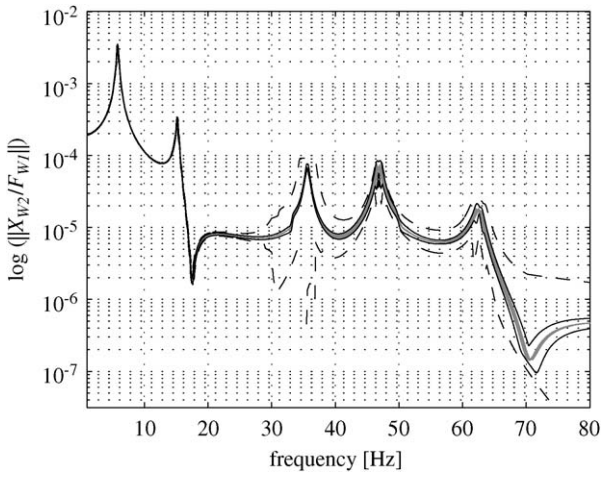

Fig. 6. Damped interval FRF of the Garteur aircraft model with the thickness of the visco-elastic layer as uncertain parameter (MR: dashed, MRE: solid).

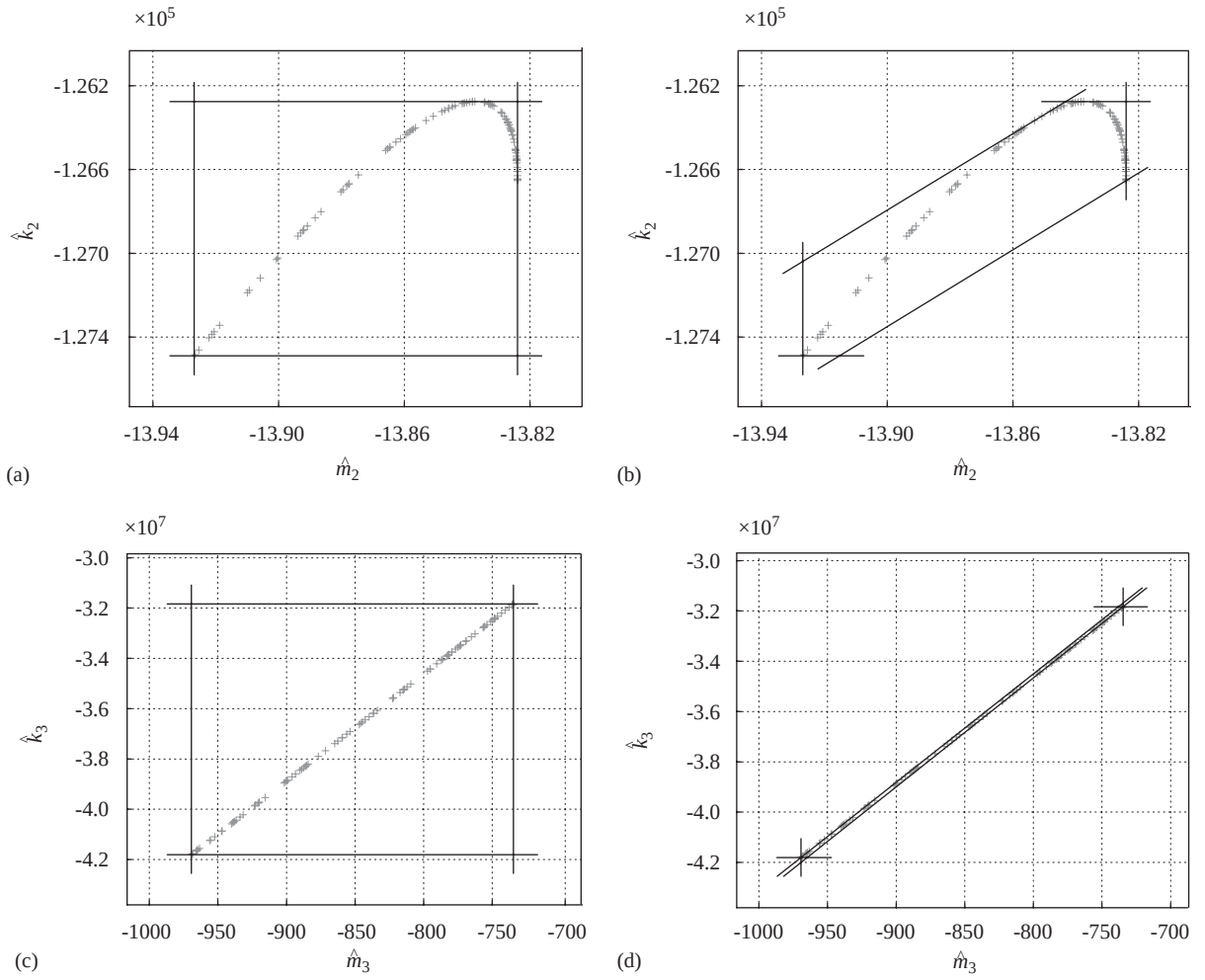

Fig. 7. Comparison of the $\langle \hat{k}_i, \hat{m}_i \rangle$-domain approximations between the MR and the MRE method: (a) $\langle \hat{k}_2, \hat{m}_2 \rangle$-domain approximation, MR method; (b) $\langle \hat{k}_2, \hat{m}_2 \rangle$-domain approximation, MRE method; (c) $\langle \hat{k}_3, \hat{m}_3 \rangle$-domain approximation, MR method; and (d) $\langle \hat{k}_3, \hat{m}_3 \rangle$-domain approximation, MRE method.

and the fuselage and the Young's modulus of the wing material (cf. Section 3.1). The proportional damping coefficients have the same values as in the previous damped analysis. Fig. 9 presents the results of the interval FRF calculation with both the MR and the MRE method, compared with results of a MCS with 1000 samples. For all uncertain parameters uniform probability density functions over the uncertainty interval are chosen. Also here, the reduction of the conservatism by the MRE approach due to the less conservative approximation of the modal domains, is clearly visible. The figure also reveals that in some frequency regions the MRE envelope FRF is still quite conservative with respect to the samples and does not give a narrow circumscription of the Monte Carlo samples, particularly in the frequency range between 44 and 48 Hz and between 59 and 80 Hz. However, a MCS with a uniform distribution on the logarithm of the stiffness of the connection springs results in a much better correspondence in these frequency regions, as

Table 3
Eigenfrequency intervals of the first 14 modes of the Garteur aircraft model with the thickness of the visco-elastic layer as uncertain parameter

Mode	Eigenfreq. interval (Hz)	Mode	Eigenfreq. interval (Hz)
1	[5.7989 ; 5.8324]	8	[54.003 ; 54.076]
2	[15.201 ; 15.234]	9	[62.290 ; 62.836]
3	[33.052 ; 33.130]	10	[67.594 ; 67.597]
4	[33.174 ; 33.262]	11	[100.22 ; 100.27]
5	[35.585 ; 35.660]	12	[128.73 ; 129.19]
6	[46.577 ; 47.078]	13	[137.10 ; 138.95]
7	[49.821 ; 49.825]	14	[150.70 ; 151.79]

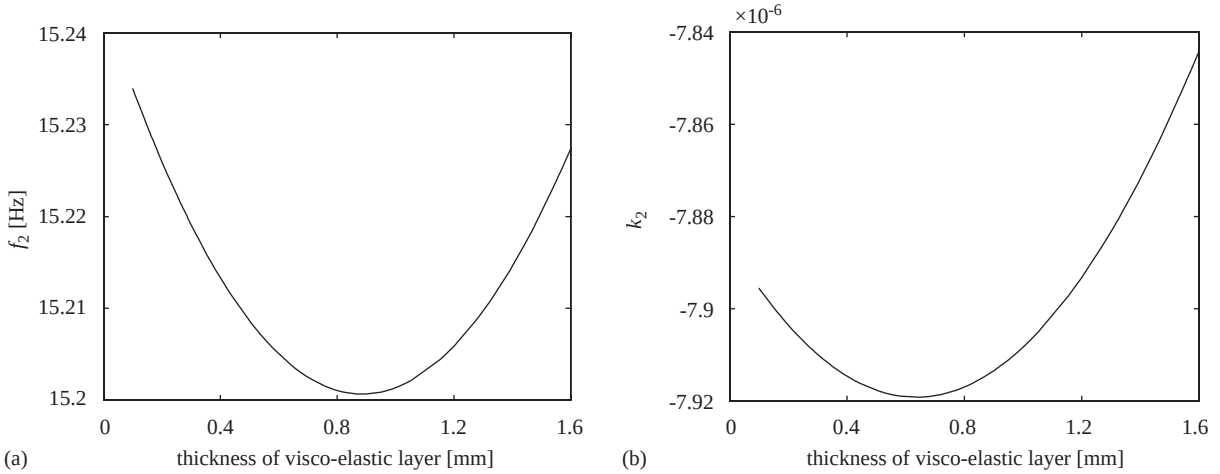

Fig. 8. Non-monotonous behaviour of modal parameters of mode 2: (a) variation of the eigenfrequency of mode 2 wrt the thickness of the visco-elastic layer; (b) variation of the modal stiffness of mode 2 wrt the thickness of the visco-elastic layer.

illustrated in Fig. 10. The samples of this MCS cover the actual stiffness interval more accurately, especially in the range of the low stiffness values. With a linear interval $k = [10; 10^{15}]$ low stiffness values have insufficient weight in MC sampling. With a logarithmic interval $\log k = [1; 15]$ a uniform distribution is closer to the actual range of the physical parameter dependency.

Fig. 10 clearly shows that the damped IFE FRF analysis using the MRE strategy is capable of giving a very close approximation of the FRF range, for different types of uncertain parameters, independent of the size and the character of the uncertainty intervals. The total number of deterministic FE analyses required to calculate the MRE interval FRF bounds is 600.

The interval FRF analysis with the MRE method gives a clear view of the combined effect of the three uncertainties on the eigenfrequencies and the FRF. This influence is most pronounced in the frequency regions 44–48 Hz and 59–80 Hz. This means that mainly modes 6 and 9 are affected by the uncertain parameters. A smaller influence is observed in the lower frequency domain.

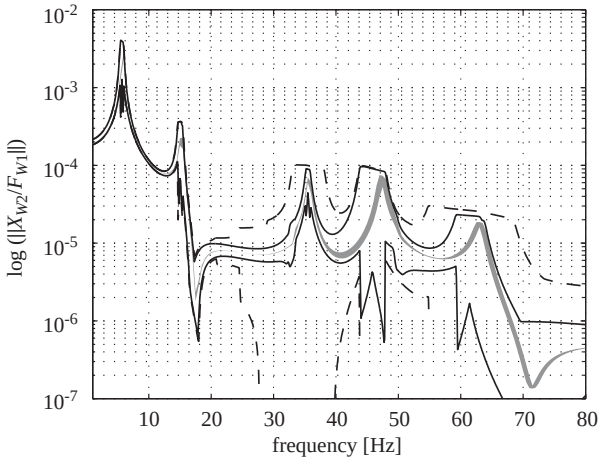

Fig. 9. Damped interval FRF of the Garteur model: MR (dashed) versus MRE (solid) method, compared with 1000 uniformly distributed Monte Carlo samples (gray lines).

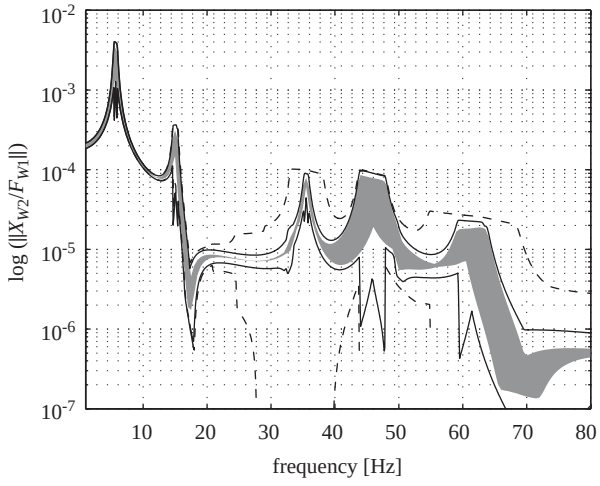

Fig. 10. Damped interval FRF of the Garteur model: MR (dashed) versus MRE (solid) method, compared with 1000 samples of alternative sampling strategy (gray lines).

3.4. Fuzzy FRF analysis with three uncertain parameters

Finally, a fuzzy FRF analysis has been performed for the Garteur aircraft model. Fig. 11 shows the triangular membership functions for the three uncertain parameters. For the thickness of the visco-elastic layer a non-symmetric membership function is used, while for the stiffness of the connection springs a triangular membership function of the logarithm of the stiffness is used. For this last uncertain parameter, the interval at the α-level equal to zero is taken to be narrower than

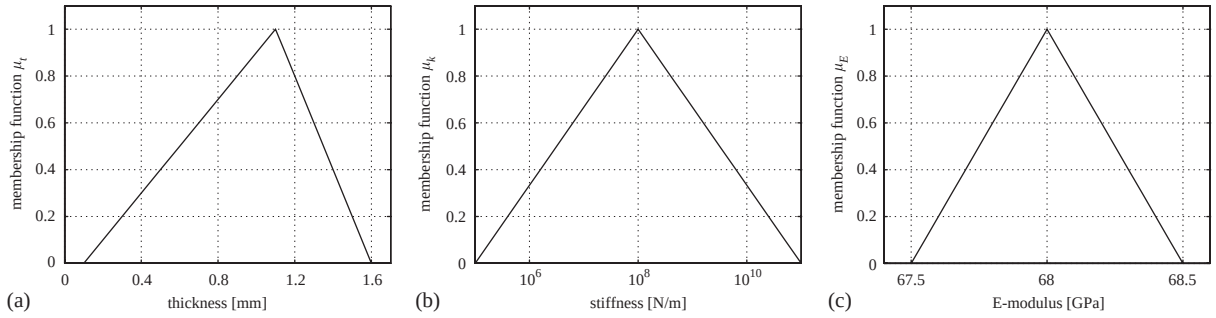

Fig. 11. Membership functions for the three uncertain parameters of the Garteur aircraft model: (a) thickness of the visco-elastic layer; (b) stiffness of the connection springs; (c) E-modulus of the wing material.

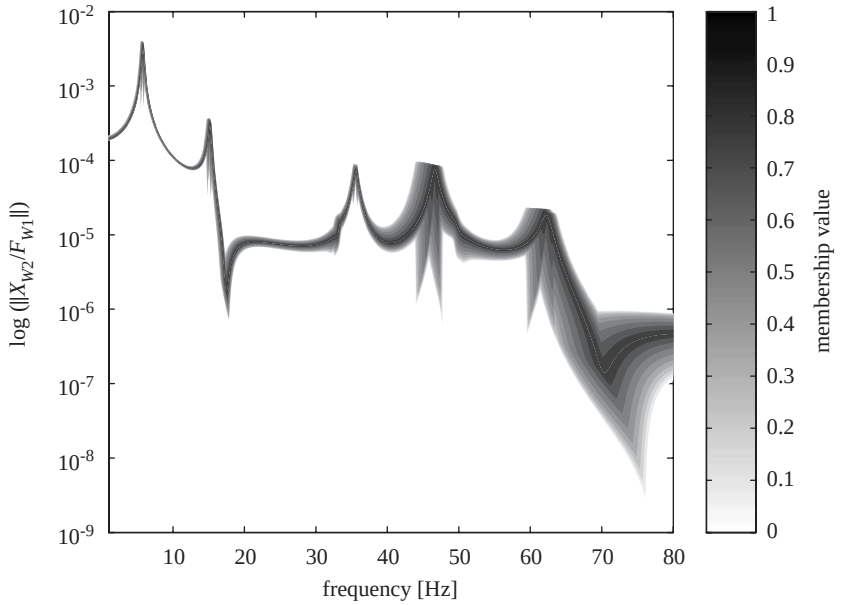

Fig. 12. Fuzzy FRF of the Garteur model with three uncertain parameters.

in the initial model, as an analysis with only the spring stiffness as uncertain parameter has revealed that the change of the stiffness outside the range of 10^6–10^{10} N/m has no influence on the modal parameter ranges $\langle \hat{k}_i \rangle$, $\langle \hat{m}_i \rangle$ and $\langle f_i \rangle$.

Fig. 12 illustrates the damped fuzzy FRF resulting from an IFE envelope FRF solution procedure at 11 α-levels. The proportional damping coefficients have the same values as in the previous damped analyses. The figure gives a clear indication of the sensitivity of both the upper and the lower damped FRF bound with respect to the input uncertainty level. The fuzzy FRF analysis reveals that the width of the uncertainty intervals mainly affects the interval FRF bounds in the frequency ranges 40–50 Hz and 60–80 Hz. For the calculation of the interval FRFs on the 11 α-levels, a total number of 2373 deterministic FE analyses have been performed.

4. Case study III: solar panel with geometric uncertainties

4.1. Problem description

This test case is a single panel in a satellite solar array, in the stowed condition. A full solar array wing consists of a series of articulated panels that are stowed during launch, and that unfold in orbit. During launch, the panels are firmly attached to the satellite structure in a number of holddown points. Load input is a base excitation, with vibrations of the launcher transmitted to the solar array through the satellite. Design criteria are applied on the magnitude of transverse displacements of the panel tips, with tips of adjacent panels in the stack not hitting each other to avoid damage to the solar cells. Another design criterium is fatigue life of the honeycomb core during launch and ascent of the launcher. In this test case, which is kindly provided by Dutch Space, Leiden (NL), a single panel in a solar array is considered. The panel is a honeycomb structure with six stiffened areas around the holddown points. In these stiffened areas, the density of the honeycomb core is higher to withstand local loads. An important problem encountered during the design phase of the solar panel is the sizing of the diameter of these denser areas, with the potting compound. Two conflicting design criteria have to be considered. On the one hand, since during launch panels of the folded array are closely held together, the tip displacements must be kept within allowable bounds in order to avoid damage to the solar cells. This design criterium can be achieved by enlarging the stiff potting compound zones. On the other hand, as the material of these stiffened zones is 4.5 times heavier than the surrounding material, the potting compound zones should not be oversized, in order to keep the weight of the satellite as low as possible.

To find a compromise between the two design criteria, the influence of the diameter of these potting compound zones on the dynamic displacements of the tips of a single panel of the folded structure is investigated.

The FE model, developed by Dutch Space, consists of a $2.25\,\mathrm{m} \times 2.732\,\mathrm{m}$ panel built with 916 composite plate elements, and it contains 6018 dofs. In Fig. 13 the six potting compound zones can be recognised as the six circular zones. The variation of the diameter of the stiffened zones has been modelled in the FE model by a number of successive concentric rings of plate elements. By changing the material properties of these plate elements, the diameter of the stiff potting compound zones is altered in a discrete way. In a first analysis, a damped interval FRF analysis, the diameters of the potting compound zones are assumed to vary independently between 119 and 190 mm. In the second analysis, a fuzzy FRF analysis, the uncertainty interval is enlarged to [119; 261] mm to show the capability of the fuzzy FRF method to handle large uncertainty intervals.

4.2. Damped interval FRF analysis

A damped interval FRF analysis is performed with the tip displacement of the solar panel as response quantity while the dynamic force is introduced as an imposed displacement base excitation perpendicular to the panel (cf. Fig. 13). The imposed displacement load is specified using the large mass method. During the analysis the first 20 modes are taken into account, covering a frequency range up to 240 Hz. The proportional damping coefficients α_K and α_M have values of 10^{-6} and 0.2, respectively, resulting in damping ratios around 0.1% for all considered modes. The MRE method is applied on this model, resulting in the upper bound on the FRF as

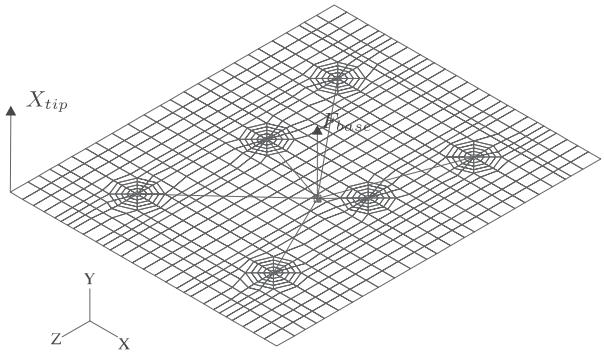

Fig. 13. Finite element model of a single panel of the folded structure (model development by Dutch Space).

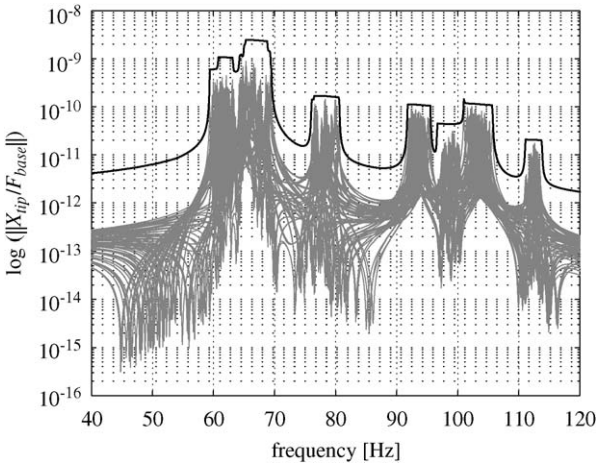

Fig. 14. Damped interval FRF of the solar panel tip due to a base excitation.

indicated in Fig. 14. The eigenfrequency intervals used in the MRE method are listed in Table 4. As the variation of the uncertain parameters which are dealt with, is modelled in a discrete way, a MCS is less applicable. Therefore, the reference FRFs for this case study do not result from a MCS, but from a vertex analysis. Considering the six potting compound zones independently, this vertex analysis gives $2^6 = 64$ FRFs which are compared to the MRE upper bound in Fig. 14.

A good correspondence can be seen in the eigenfrequency ranges 59–70, 76–80, 92–106 and 111–114 Hz. In between the resonance peaks of the FRF, the amount of conservatism is considerable. This conservatism is mainly due to the large size of the uncertainty interval: a variation of 46% is considered. In this case, this large uncertainty interval causes a large shift of nodal and anti-nodal positions of the eigenmodes in the response area, and consequently a large amount of switch modes. A conservative approximation of response levels is a feature of the proposed method. In this test case, this phenomenon is pronounced in frequency ranges between resonance peaks. The individual modal envelope FRFs are conservative, resulting in an

Table 4
Eigenfrequency intervals of the solar panel model

Mode	Eigenfreq. interval (Hz)	Mode	Eigenfreq. interval (Hz)
1	[59.383 ; 63.171]	11	[133.94 ; 137.38]
2	[60.762 ; 64.568]	12	[140.09 ; 143.52]
3	[64.228 ; 68.796]	13	[145.15 ; 153.05]
4	[65.011 ; 69.293]	14	[155.84 ; 159.52]
5	[65.264 ; 69.480]	15	[165.70 ; 169.95]
6	[76.050 ; 80.528]	16	[187.30 ; 187.90]
7	[91.798 ; 95.504]	17	[204.48 ; 211.13]
8	[96.637 ; 100.98]	18	[211.70 ; 218.51]
9	[100.98 ; 105.66]	19	[216.99 ; 218.85]
10	[111.10 ; 113.76]	20	[230.44 ; 233.51]

overestimation of the upper FRF bound as can be seen in Fig. 14. Furthermore, the large uncertainty interval causes the eigenfrequency intervals of different modes to overlap. It should be stressed that the conservatism is mainly situated between the FRF peaks. The resonance behaviour at the different eigenfrequency regions is narrowly predicted, which is the most important in most of the industrial applications.

The total number of deterministic FE analyses required to calculate the MRE interval FRF bounds, taking into account 20 modes, is 440.

4.3. Damped fuzzy FRF analysis

A fuzzy FRF analysis has been performed for the solar panel with the six potting compound zones as uncertain parameters. The proportional damping coefficients α_K and α_M have values of 10^{-5} and 11, respectively, resulting in damping ratios between 1.1% and 1.9% for all considered modes. Fig. 15 shows the membership function that is used for all six stiffened zones. The uncertainty interval on the diameter of the stiffened zones at the α-level equal to zero is enlarged to [119; 261] mm. The resulting fuzzy FRF of the tip displacement of the panel is shown in Fig. 16. Only the membership evolution of the upper bound of the FRF is illustrated as the lower bound is very small for a large part of the frequency domain. The figure clearly shows the evolution of the tip displacement with respect to the size of the design uncertainty interval on the dimension of the stiffened zones. In this case, the resonances in the region around 65 Hz clearly determine the maximum response level that can be reached in the observed frequency domain. The fuzzy analysis in this case reveals that exactly in this region, the impact of the introduced uncertainty is relatively high. This means that the designer can base the choice of the diameter of the potting compound zones on the fuzzy FRF by selecting an acceptable response level. The maximal membership value that is reached for this response level over the analysed frequency domain determines the acceptable α-level. Based on the principle of the α-level strategy (see part 1 of this paper), the designer now can conclude that choosing the diameter of the stiffened zones inside the corresponding interval on the input membership function will lead to a safe design.

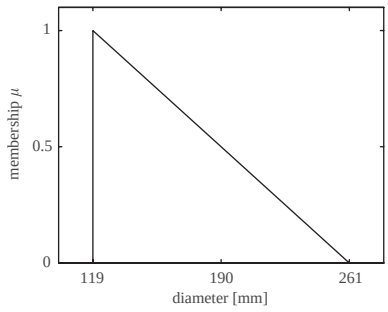

Fig. 15. Membership function for the diameter of the potting compound zones of the solar panel.

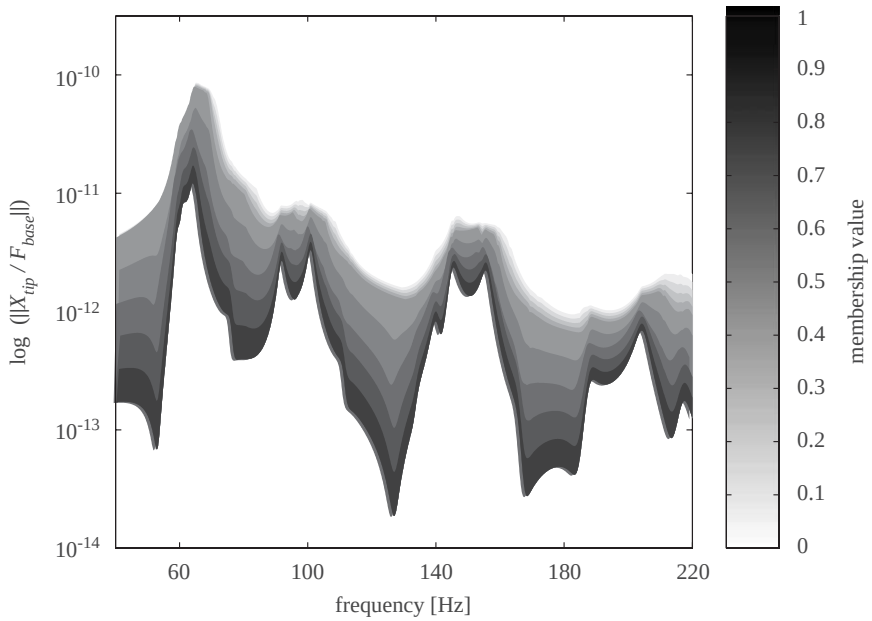

Fig. 16. Damped fuzzy FRF (upper bound) of a single solar panel.

5. Case study IV: COROT baffle cover

5.1. Problem description

In this section the influence of physical uncertainties on the dynamic behaviour of the telescope baffle cover (Fig. 17) for the COROT mission (Seismology of Stars: Convection and Rotation) is investigated. The cover prototype consists of a sandwich circular plate interfacing the baffle wall by means of two arms and compression springs [10]. The diameter of the cover is 832 mm, the thickness 22.7 mm. The FE model of this structure is built by Centre Spatial de Liège (B). It contains 964 nodes and 1042 elements. For the cover lid laminate plate elements are used. Both the hinge and the lock arm are modelled with beam elements and plate elements. Linear springs

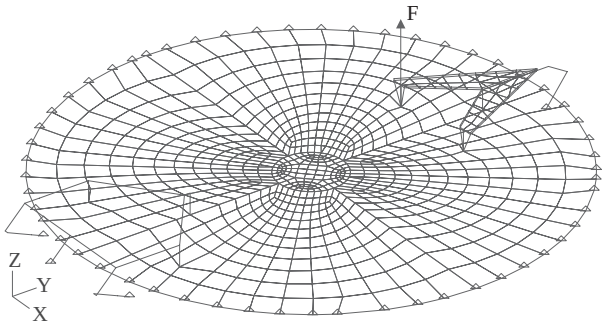

Fig. 17. Finite element model of the cover with the hinge arm (left) and the lock arm (right) (model development by Centre Spatial de Liège).

Table 5
Uncertain parameters of the COROT baffle cover

Uncertain parameter	Unit	Nominal value	Uncertainty interval
Launch lock side arm preload stiffness	N/mm	203	[198 ; 208]
Hinge side arm preload stiffness	N/mm	99	[96 ; 102]
Hinge torsion stiffness	Nmm	1000	[975 ; 1025]
Cover lid non-structural mass	g/mm^2	3.7×10^{-4}	[2.96 ; 4.44] $\times 10^{-4}$
Sandwich skin thickness	mm	0.35	[0.34 ; 0.36]
Honeycomb thickness	mm	22.0	[21.8 ; 22.2]

connect the nodes on the edge of the cover with nodes on the baffle which are clamped. In this way the springs model the boundary condition of simple support with no sliding assumed to the cover lid in contact with the baffle.

Six uncertain parameters are identified, as listed in Table 5. The first three uncertainties arise from a variability of 5% on the stiffness of the compression springs. The uncertainty on the use of screws, washers and nuts is modelled by the range of the cover lid non-structural mass (NSM). Typical production tolerances are considered on the thickness of the sandwich skins and the honeycomb core.

5.2. Eigenfrequency interval analysis

During launch of spacecraft, different types of vibrations are excited in a wide frequency spectrum, to which all structural and non-structural components and equipment are subjected. For satellites and space instrumentation, it is very important that these vibrations do not excite important resonances, as they can cause damage to these delicate and expensive structures. Therefore, strict design criteria regarding the eigenfrequencies are often imposed on the design of such space structures and instrumentation. Consequently, in the design phase where not all properties are yet defined, it is of utmost importance to investigate the influence of uncertainties on the eigenfrequency ranges.

Table 6
Eigenfrequency intervals of the first 10 modes of the COROT baffle cover

Mode	Eigenfreq. interval (Hz)	Mode	Eigenfreq. interval (Hz)
1	[191.30 ; 199.66]	6	[490.59 ; 500.61]
2	[278.47 ; 282.71]	7	[517.89 ; 538.59]
3	[360.52 ; 367.48]	8	[638.71 ; 650.70]
4	[462.51 ; 462.59]	9	[667.19 ; 678.98]
5	[462.73 ; 465.25]	10	[702.54 ; 715.87]

In this section the influence of the uncertain parameters of Table 5 on the eigenfrequencies of the COROT baffle cover is investigated. Table 6 lists the eigenfrequency intervals resulting from a global optimisation procedure for the first 10 modes. Clearly, the first eigenfrequency as well as the eigenfrequencies of modes 6–10 are strongly affected by the uncertain parameters. Therefore special attention has to be paid to the specification of property values and the control on production tolerances if strict design criteria have to be met.

5.3. Damped interval FRF analysis of the cover lid

The influence of the uncertain parameters on a damped direct FRF is investigated. Both the excitation and the response are considered in one of the two nodes of the cover lid that rigidly connect the cover lid with the lock arm, as indicated in Fig. 17. The first 20 modes are taken into account in the analysis, covering a frequency range up to 1300 Hz. The values of the proportional damping coefficients α_K and α_M are, respectively, 4×10^{-6} and 25, resulting in damping ratios between 1.0% and 1.7% for all considered modes.

Figs. 18 and 19 show the amplitude and the phase of the damped interval FRF, compared to 500 Monte Carlo samples. The dashed line represents the envelope FRF calculated with the MR method, whereas the solid line represents the envelope FRF calculated with the MRE method. The figures clearly prove the benefits of the MRE method with respect to the MR method, as the conservatism on the envelope FRF is substantially decreased for almost the entire frequency range. A somewhat larger amount of conservatism remains in the frequency region around 900 Hz. This conservatism is caused by the modal overlap of modes 14–18.

The total number of deterministic FE analyses required to calculate the MRE interval FRF bounds is 448. In this case study, all modal parameters behave in a monotonic way with respect to the uncertain parameters. Consequently, the modal parameter ranges $\langle \hat{k}_i \rangle$, $\langle \hat{m}_i \rangle$ and $\langle f_i \rangle$ are correctly predicted by the vertex method.

5.4. Fuzzy FRF analysis of the cover lid

A fuzzy FRF analysis of the COROT baffle cover is performed with enlarged uncertainty intervals. For all uncertain parameters, the uncertainty interval is taken twice as wide, except for the uncertainty interval on the non-structural mass of the cover lid that is 1.5 times the original interval. All membership functions are triangular and symmetric. Fig. 20 presents the results of

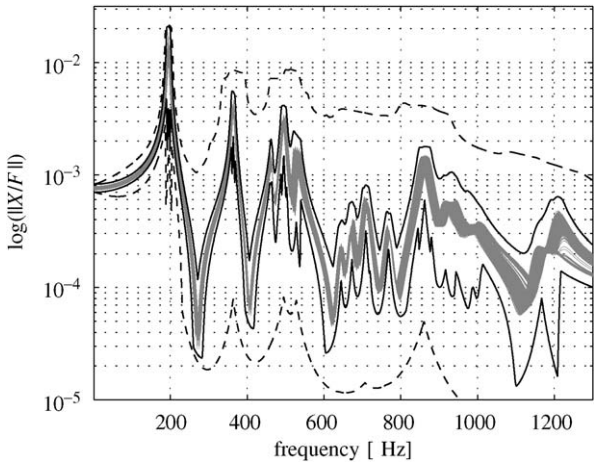

Fig. 18. Amplitude of the damped interval direct FRF of the COROT baffle cover (MR: dashed, MRE: solid).

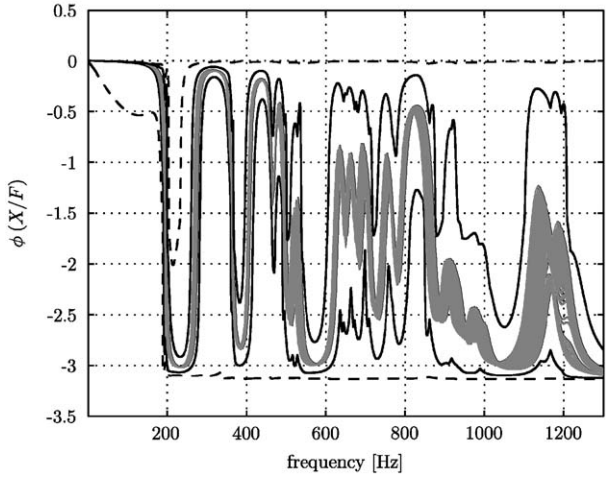

Fig. 19. Phase of the damped interval direct FRF of the COROT baffle cover (MR: dashed, MRE: solid).

the fuzzy FRF analysis with 11 α-levels. The values of the proportional damping coefficients are the same as in the previous analysis. The figure gives a clear indication of the effect of the width of the input uncertainty intervals on the FRF envelopes. In this case, the fuzzy FRF shows that the effect of the uncertainties on the maximal response level reached in the observed frequency region is rather limited. This means that the analysed design is robust with respect to the defined model uncertainties. On the other hand, the effect of the uncertainties on the eigenfrequencies is more expressed. If the design specifications are given in terms of eigenfrequencies, this fuzzy eigenfrequency behaviour can be very useful information for a designer. Based on the α-level strategy (similar as for the previous case study), an acceptable membership level can be derived in

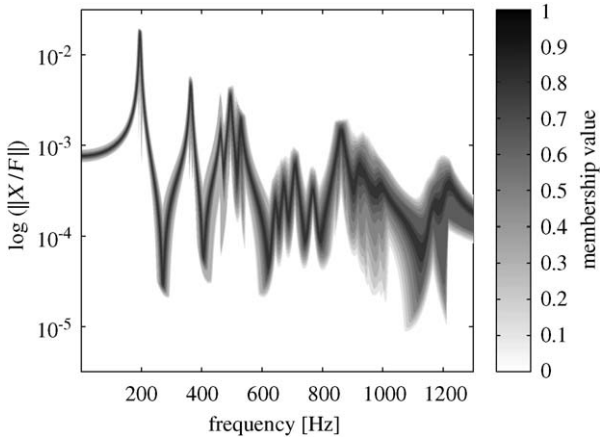

Fig. 20. Fuzzy FRF of the cover lid with six uncertain parameters.

order to keep a certain eigenfrequency within given bounds. Using the corresponding input intervals as tolerances will yield a safe design.

6. Conclusions

This paper demonstrates the applicability of the IFE and the FFE method for dynamic analysis of structures with different types of uncertain parameters through four case studies. A plate model with uncertain boundary conditions, the Garteur aircraft model, a solar panel with geometric uncertainties and the cover of the COROT telescope baffle are presented.

The IFE method proves to be powerful and reliable: a conservative approximation of the upper and lower bounds of an FRF is calculated in a single run. For these particular cases a MCS proves to be inappropriate for envelope FRF analysis since the obtained set of response functions is very sensitive to the choice of the PDFs on the input interval.

The different case studies clearly prove the benefits of the MRE method with respect to the MR method for damped structures. The MRE method gives a tight approximation of the actual response range, as the conservatism, introduced by the assumption of independency between the modal mass and stiffness, is reduced significantly. Whereas the MR method provides fair results for the lowest modes only, the advantage of the MRE strategy is evident at increasing frequency. In the future, special attention will be paid on the further reduction of the conservatism introduced by the IFE method for FRF analysis, especially in the case of switch modes. Also the influence of modal overlap on the envelope FRFs will be investigated.

The examples further show the difference between interval analysis and fuzzy analysis. Interval analysis only predicts the bounds on responses. Fuzzy response quantities also show the effect of parameter variations on the output. The fuzzy FRF gives a clear indication of the variation of the worst-case response with the considered input uncertainty bounds. It gathers information on the response sensitivity to the input uncertainties over the complete frequency domain in a single graphical representation.

Acknowledgements

The research on the solar panel and the COROT baffle cover was funded by the Belgian federal government via the Federal Office for Scientific, Technical and Cultural Affairs (Federale Diensten voor Wetenschappelijke, Technische en Culturele Aangelegenheden, DWTC, project TAP31: *Static and dynamic design analysis procedures for structures with uncertain parameters*). The test case of the solar panel was kindly made available by J. Wijker of Dutch Space, Leiden (NL). The test case of the COROT baffle cover was made available by P. Rochus of Centre Spatial de Liège (B).

H. De Gersem is research assistant of the Fund for Scientific Research - Flanders (Belgium) (F.W.O.-Vlaanderen). The research of D. Moens is funded by a post-doctoral fellowship from the Institute for the promotion of Innovation by Science and Technology in Flanders (IWT - Vlaanderen), Brussel.

References

[1] D. Moens, D. Vandepitte, An interval finite element approach for the calculation of envelope frequency response functions, *International Journal for Numerical Methods in Engineering* 61 (14) (2004) 2480–2507.

[2] D. Moens, A Non-Probabilistic Finite Element Approach for Structural Dynamic Analysis with Uncertain Parameters, *Ph.D. Thesis*, Katholieke Universiteit Leuven, October 2002.

[3] W. Oberkampf, S. DeLand, B. Rutherford, K. Diegert, K. Alvin, A new methodology for the estimation of total uncertainty in computational simulation, *Proceedings of the 40th AIAA/ASME/ASCE/AHS/ASC Structures, Structural Dynamics and Materials Conference, AIAA-99-1612*, 1999, pp. 3061–3083.

[4] K. Alvin, W. Oberkampf, K. Diegert, B. Rutherford, Uncertainty quantification in computational structural dynamics: a new paradigm for model validation, *Proceedings of the 16th International Modal Analysis Conference, IMAC XVI*, 1998, pp. 1191–1197.

[5] M. Hanss, K. Willner, A fuzzy arithmetical approach to the solution of finite element problems with uncertain parameters, *Mechanics Research Communications* 27 (3) (2000) 257–272.

[6] S. Donders, J. Van de Peer, S. Dom, H. Van der Auweraer, D. Vandepitte, Parameter uncertainty and variability in the structural dynamics modeling process, *Proceedings of the 22nd International Modal Analysis Conference, IMAC XXII*, 2004.

[7] M. Degener, M. Hermes, Ground vibration test and finite element analysis of the GARTEUR SM-AG19 testbed, Technical Report IB 232-96 J 08, DLR - German Aerospace Research Establishment, Institute for Aeroelasticity, October 1996.

[8] M. Friswell, New measurements on the GARTEUR testbed, Technical Report of the Garteur Action Group, University of Wales Swansea, UK, December 2000.

[9] P. Neven, Definition of basic test cases: material uncertainties, geometrical uncertainties, uncertain boundary conditions (B) in mechanical engineering, TAP 31 Report Part 1.4, February 2004.

[10] G. Rodrigues, COROT baffle cover FEM description, ESTEC Technical Note, TOS-MCS/2002, draft version, December 2002.